© 2018. Published by The Company of Biologists Ltd | Development (2018) 145, dev164962. doi:10.1242/dev.164962

RESEARCH REPORT

Regulation of xylem fiber differentiation by gibberellins through DELLA-KNAT1 interaction

Amelia Felipo-Benavent[1], Cristina Úrbez[1], Noel Blanco-Touriñán[1], Antonio Serrano-Mislata[1], Nicolas Baumberger[2], Patrick Achard[2], Javier Agustí[1], Miguel A. Blázquez[1,*] and David Alabadí[1]

ABSTRACT

The thickening of plant organs is supported by secondary growth, a process by which new vascular tissues (xylem and phloem) are produced. Xylem is composed of several cell types, including xylary fibers, parenchyma and vessel elements. In *Arabidopsis*, it has been shown that fibers are promoted by the class-I KNOX gene *KNAT1* and the plant hormones gibberellins, and are repressed by a small set of receptor-like kinases; however, we lack a mechanistic framework to integrate their relative contributions. Here, we show that DELLAs, negative elements of the gibberellin signaling pathway, physically interact with KNAT1 and impair its binding to KNAT1-binding sites. Our analysis also indicates that at least 37% of the transcriptome mobilized by KNAT1 is potentially dependent on this interaction, and includes genes involved in secondary cell wall modifications and phenylpropanoid biosynthesis. Moreover, the promotion by constitutive overexpression of *KNAT1* of fiber formation and the expression of genes required for fiber differentiation were still reverted by DELLA accumulation, in agreement with post-translational regulation of KNAT1 by DELLA proteins. These results suggest that gibberellins enhance fiber development by promoting KNAT1 activity.

KEY WORDS: Hormones, Plant vasculature, Secondary cell wall, Lignin

INTRODUCTION

How the environment regulates the development of multicellular organisms is a fundamental issue in biology about which little is known. Gibberellins (GAs) are plant hormones that integrate environmental information and translate it into developmental outputs (i.e. by promoting developmental transitions or initiating specific differentiation programs). For example, in many plant species, GA levels increase in seeds when exposed to appropriate light, temperature and humidity conditions, and such an increase is a trigger for mobilization of nutrient resources and growth of the previously dormant embryo (Shu et al., 2016). Similarly, GAs are necessary to establish the morphogenesis of trichomes (specialized epidermal cells with attributed functions in pathogen resistance) (Pattanaik et al., 2014).

From a mechanistic perspective, GA signaling is initiated by binding of GAs to the GA receptor, which then recognizes and promotes the degradation of DELLA proteins assisted by F-box proteins (Daviere and Achard, 2013; Hirano et al., 2008; Schwechheimer, 2011). In *Arabidopsis*, it has been shown that DELLA proteins act as transcriptional regulators by directly interacting with specific transcription factors that, owing to such interaction, alter their function (Locascio et al., 2013b; Marin-de la Rosa et al., 2014). Based on the identification of DELLA interactors (over 60 are known so far) and the characterization of the impact of particular interactions in development, we are beginning to understand the molecular mechanisms by which GAs regulate specific developmental processes. Clear examples of these are the control of the meristematic activity in the root via the interaction of DELLAs with B-type ARRs (Marin-de la Rosa et al., 2015); the transition to the reproductive phase through the DELLA-SPL transcription factors interaction (Yu et al., 2012); or the control of germination through the interaction of DELLA proteins with ABI3, ABI5, AtML1, and TCP14 and TCP15 (Lim et al., 2013; Resentini et al., 2015; Rombolá-Caldentey et al., 2014). However, GAs are also central to many other developmental processes in which the molecular mechanisms underlying their activity remain unknown. A remarkable example is the regulation of vascular development.

Plant vasculature originates during embryogenesis, but its development is not restricted to that stage. Indeed, depending on the environmental conditions or on the specific necessities that plants may encounter, vascular development can stop and resume multiple times during the plant life cycle. In adult plants, most of the new vascular cells are derived from the cambium, a specialized pool of undifferentiated meristematic cells that is programmed to develop exclusively the vascular tissues, namely xylem and phloem, that conduct water and solutes, and the assimilates, respectively. GAs have been shown to promote at least two aspects of vascular development: xylem expansion and the differentiation of a specific cell type within the xylem – the xylem fibers (Aloni, 2013; Eriksson et al., 2000; Mauriat and Moritz, 2009; Ragni et al., 2011). Here, we focus on the molecular mechanism underlying the activity of the GAs in xylem fiber differentiation. Recent discoveries indicate that KNOX-I genes [*KNAT1/BREVIPEDICELLUS* and *SHOOTMERISTEMLESS* (*STM*)] promote xylem fiber differentiation during vascular development (Liebsch et al., 2014) and that GA-dependent promotion of fiber differentiation, indeed, depends on the presence of active KNAT1 (Ikematsu et al., 2017). Importantly, we have identified KNAT1 as an interactor of the *Arabidopsis* DELLA protein GAI. In such a conceptual framework, we have tested the hypothesis that the function of GAs in the regulation of fiber development is regulated by the DELLA-KNAT1 physical interaction.

RESULTS AND DISCUSSION

Using a previously described yeast two-hybrid (Y2H) screen with the GRAS domain of the DELLA protein GAI ('M5-GAI') as bait, we identified a number of putative DELLA interactors (Locascio

[1]Instituto de Biología Molecular y Celular de Plantas (CSIC-Universidad Politécnica de Valencia), Valencia 46022, Spain. [2]Institut de Biologie Moléculaire des Plantes (CNRS-Université de Strasbourg), Strasbourg 67084, France.

*Author for correspondence (mblazquez@ibmcp.upv.es)

C.U., 0000-0001-9345-7322; N.B-T., 0000-0003-4610-6110; A.S., 0000-0002-8828-1809; P.A., 0000-0003-0520-7839; J.A., 0000-0003-4610-6110; M.A.B., 0000-0001-5743-0448; D.A., 0000-0001-8492-6713

Received 23 February 2018; Accepted 29 October 2018

Development (2018) 145, dev164962. doi:10.1242/dev.164962

et al., 2013a), among which KNAT1/BREVIPEDICELLUS(BP) was present. KNAT1/BP belongs to the KNOX family of transcription factors (which are general regulators of plant development) and has been shown to regulate the activity of the shoot apical meristem and the cambium (Byrne et al., 2002; Liebsch et al., 2014; Lincoln et al., 1994). To corroborate the observed DELLA-KNAT1 interaction and, at the same time, to map the interacting domains of GAI with KNAT1, we expanded the Y2H assay by including several truncated versions of the GAI clone as bait (Fig. 1A) and another DELLA protein, RGA (Fig. S1). Results showed that only the full-length and the M5 versions (but not the other truncated versions) of GAI, as well as the M5-like version of RGA, were able to interact with KNAT1 (Fig. 1A and Fig. S1). This result resembles the interactions with other transcription factors, i.e. with BZR1, PIF4 or JAZ1 (de Lucas et al., 2008; Gallego-Bartolomé et al., 2012; Hou et al., 2010), and indicates that the LR1 domain of the protein is necessary, but not sufficient, for the GAI-KNAT1 interaction. We also verified the interaction between GAI and KNAT1 *in planta* by co-immunoprecipitation studies in *Nicotiana benthamiana* leaves (Fig. 1B; Fig. S2).

DELLA interaction with transcription factors has been shown to either impair their ability to bind their target cis elements (de Lucas et al., 2008; Gallego-Bartolomé et al., 2012) or to promote target transactivation (Fukazawa et al., 2014; Marin-de la Rosa et al., 2015). To establish the possible molecular effect of DELLA on KNAT1, we examined the ability of KNAT1 to bind a sequence containing a previously identified KNAT1-bindng *cis* element (Fig. 2A; Mele et al., 2003), using electrophoretic mobility shift assays (EMSAs). As expected, bacterially produced KNAT1 was able to specifically bind this *cis* sequence (Fig. 2B) and, more importantly, the addition of increasing amounts of RGA competitively impaired the binding of KNAT1 to the corresponding probe (Fig. 2C). This result is in agreement with a model in which DELLAs impair the recognition by KNAT1 of its target promoters.

Given that KNAT1 plays a central role in the regulation of meristematic activity, understanding the biological meaning of the DELLA-KNAT1 interaction appears to be of general relevance for plant development. We hypothesized that KNAT1 would control different gene sets depending on the presence or absence of DELLA proteins. To test such a hypothesis and to gain more insights into the general biological significance of the DELLA-KNAT1 interaction, we performed comparative transcriptomic analyses. We first treated seedlings of the *KNAT1* overexpressor transgenic line *35S::KNAT1* (Lincoln et al., 1994) (Fig. S3) and its wild type (No-0) with

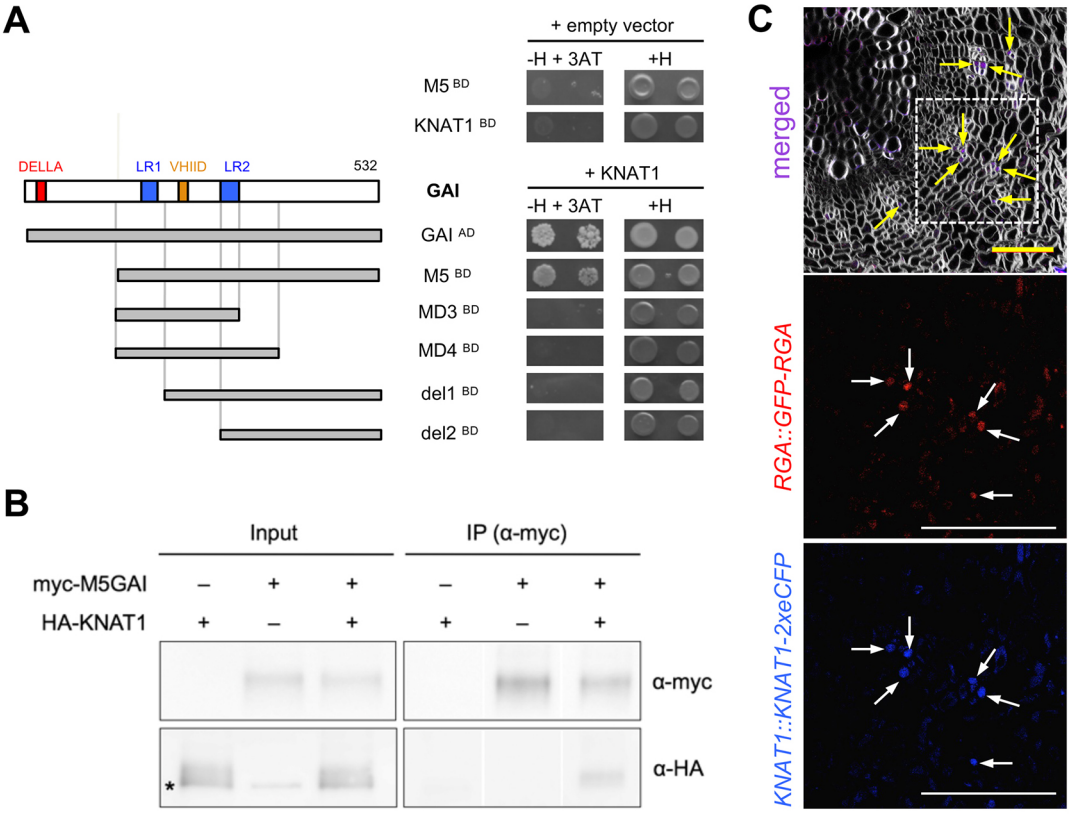

Fig. 1. KNAT1 interacts physically and colocalizes with DELLA proteins. (A) Y2H assays analyzing the interaction between KNAT1 and the full-length and deleted versions of the DELLA protein GAI (Gallego-Bartolomé et al., 2012). Two serial dilutions per yeast clone are shown. +H, control medium containing His; –H, selective medium lacking His and containing 5 mM 3-aminotriazol (3-AT). Pictures of the plates were taken after 4 days at 28°C. (B) Co-immunoprecipitation showing the interaction between c-myc-M5GAI and HA-KNAT1 in leaves of *N. benthamiana.* The recombinant proteins were expressed either alone or together. Total proteins were immunoprecipitated using anti-c-myc conjugated paramagnetic beads and were detected by immunoblotting with either anti-c-myc or anti-HA antibodies. The sizes of the bands correspond to the expected sizes of the fusion proteins. The asterisk indicates a nonspecific band. White lines indicate where the original gel (Fig. S2) has been recomposed. (C) Hand-cut section of a 28-day-old hypocotyl of *Arabidopsis thaliana* grown in 10 µM PAC showing colocalization of RGA::GFP-RGA (red) and KNAT1::KNAT1-2xeCFP (blue). Upper panel, simultaneous detection of cell walls stained with Direct Red 23 (gray), and GFP-RGA and KNAT1-2xeCFP proteins (colocalization is observed as a purple signal). High magnifications of the outlined region with single detection of GFP-RGA and KNAT1-2xeCFP are shown below. Arrows indicate nuclei where both proteins were present. Scale bars: 50 µm.

Development (2018) 145, dev164962. doi:10.1242/dev.164962

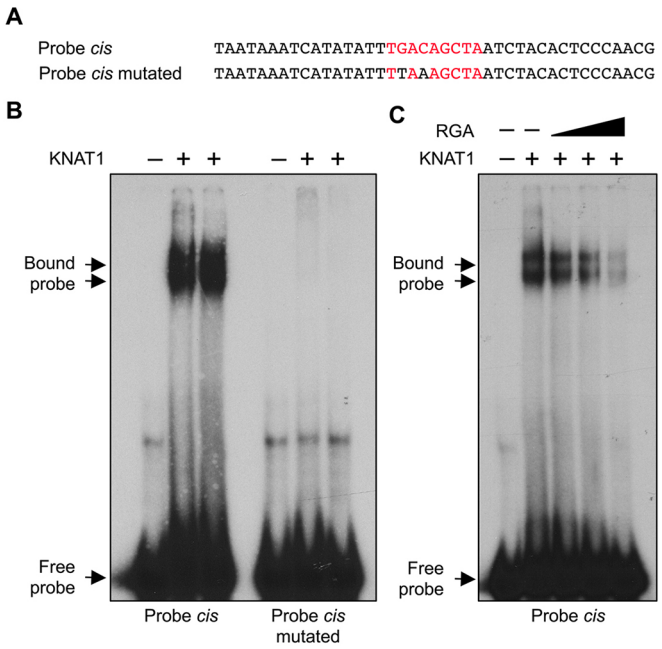

Fig. 2. RGA impairs the ability of KNAT1 to bind their target promoter. (A) Sequences of the dsDNA oligonucleotide probes used in EMSAs. The wild-type sequence corresponds to the promoter of *AT1G77530* and red indicates the previously identified KNAT1-binding site (Mele et al., 2003). (B) EMSAs using the recombinant protein KNAT1 and oligonucleotides radiolabeled with ^{32}P. Two different concentrations of recombinant KNAT1 were used (lanes 2 and 3 of each probe). (C) EMSA using the recombinant protein KNAT1 either alone or in the presence of increasing quantities of recombinant RGA (5-, 10- and 20-fold in lanes 3, 4 and 5, respectively).

paclobutrazol (PAC), an inhibitor of GA biosynthesis that induces the accumulation of DELLAs (Silverstone et al., 1998), for 18 h. At that point, seedlings of each genotype were separated into two blocks: one that was treated with GA for 5 h (to induce DELLA degradation) and another one that remained in PAC (to maintain the accumulation of DELLA). In this way, we generated four different classes of samples: (1) wild type treated with PAC; (2) *35S::KNAT1* treated with PAC; (3) wild type treated with PAC plus GA; and (4) *35S::KNAT1* treated with PAC and GA. Through immunodetection of the DELLA protein RGA, we confirmed that PAC-treated samples of each genotype contained higher levels of DELLA proteins than GA-treated samples (Fig. S4). We then performed RNA-seq transcriptomic analyses with samples of all four classes and established comparisons between the transcriptomic profiles. We compared the transcriptome of wild type with that of *35S::KNAT1* treated with PAC and, in parallel, the transcriptomes of wild type with that of *35S::KNAT1* treated with GA (Fig. 3A; Table S1). The comparison between PAC-treated samples yielded genes that are KNAT1 targets in the presence of DELLAs, whereas the comparison between PAC+GA samples yielded genes that are KNAT1 targets in the absence of DELLAs (Fig. 3A). Using a statistical level of $P<0.01$, we identified 985 genes misregulated by KNAT1 only in the presence of DELLA and 776 genes misregulated only in the absence of DELLA. Out of those, 262 and 183 did it with a fold change higher than 2 (Fig. 3B). Our results show that KNAT1 has different targets depending on the presence of DELLAs, reinforcing the hypothesis that KNAT1 plays different biological roles depending on whether it interacts with DELLA proteins or not, and suggest, therefore, that the DELLA-KNAT1 interaction is relevant.

To investigate the particular KNAT1 functions that would be modulated by DELLA-KNAT1 interaction, we focused on the genes that were differentially affected by *KNAT1* overexpression only in the absence or only in the presence of DELLAs. In both sets of genes, our Gene Ontology analysis showed a statistically significant enrichment of categories involved in cell wall metabolism, phenylpropanoid and lignin biosynthesis, and the response to hormones (Fig. S5). In fact, 63 and 78 of the genes induced and repressed by KNAT1, respectively, had been previously identified as 'cell wall-associated genes' by gene co-expression studies (Wang et al., 2012). To calibrate the involvement of KNAT1 and DELLA in this process, we then generated a co-expression network using those 141 genes as seed in the ATTED tool (Obayashi et al., 2007) and found that the KNAT1-DELLA interaction could potentially affect a total of almost 200 genes involved in secondary cell wall production, with 34 of them being differentially regulated by DELLA-dependent KNAT1 activity (Fig. 3C-E; Table S2). Thus, although KNAT1 was already known as a regulator of lignin biosynthesis (Mele et al., 2003), our results point out that some aspects of such regulation are DELLA dependent. Moreover, when we examined the expression of randomly selected SCW-related genes (Wang et al., 2012; Table S2), which had been tagged as 'KNAT1 targets' according to our RNA-seq experiment (Table S1), we found that six out of eight genes tested reproduced DELLA-dependence in mature hypocotyls undergoing secondary growth (Fig. S6), supporting the relevance of the interaction between DELLAs and KNAT1 for vascular development. In addition, this relevance was further supported by the colocalization of KNAT1-CFP and GFP-RGA in the nuclei of vascular cells of hypocotyls undergoing secondary growth (Fig. 1C). The signal was maximized when the plants were grown in the presence of 10 µM PAC.

As opposed to its role in the shoot apical meristem, where KNAT1 prevents early cell differentiation (Byrne et al., 2002), previous reports have shown that, during secondary growth, KNAT1 promotes xylem fiber differentiation (Liebsch et al., 2014; Mele et al., 2003). A recent report suggested a genetic link between KNAT1 and GA during xylem fiber differentiation, by which the developing xylem would gain the capacity to respond to GA in a KNAT1-dependent manner through a currently unknown molecular mechanism (Ikematsu et al., 2017). Having confirmed the DELLA-KNAT1 physical and functional interactions (Fig. 1; Fig. 3), we decided to test the relevance of this particular interaction in the control of xylem differentiation. We therefore treated a *knat1* loss-of-function mutant (*bp-11*) and the *35S::KNAT1*-overexpressor line (together with their respective controls, Col-0 and No-0) with GA_3 or PAC. In order to analyze the differential development of fibers across samples, hypocotyls were collected, sectioned and stained with phloroglucinol to detect lignin deposition. Similar to previous observations (Ikematsu et al., 2017), our GA treatments did not induce fiber formation in the *bp-11* mutant, but we observed that they promoted fiber differentiation in all the other genotypes (Fig. 4). *KNAT1* overexpression also promoted the formation of xylem fibers (Fig. 4), which was especially evident as the No-0 accession typically produces less fiber development than other accessions such as Col-0. More importantly, DELLA hyperaccumulation achieved with the PAC treatment completely abolished fiber production even in the *35S::KNAT1* line (Fig. 4D), and also reduced cambial activity (Fig. 4B). This result, together with the fact that *KNAT1* expression levels are not affected by GA or PAC treatments (Fig. 5), support the proposed model of

Development (2018) 145, dev164962. doi:10.1242/dev.164962

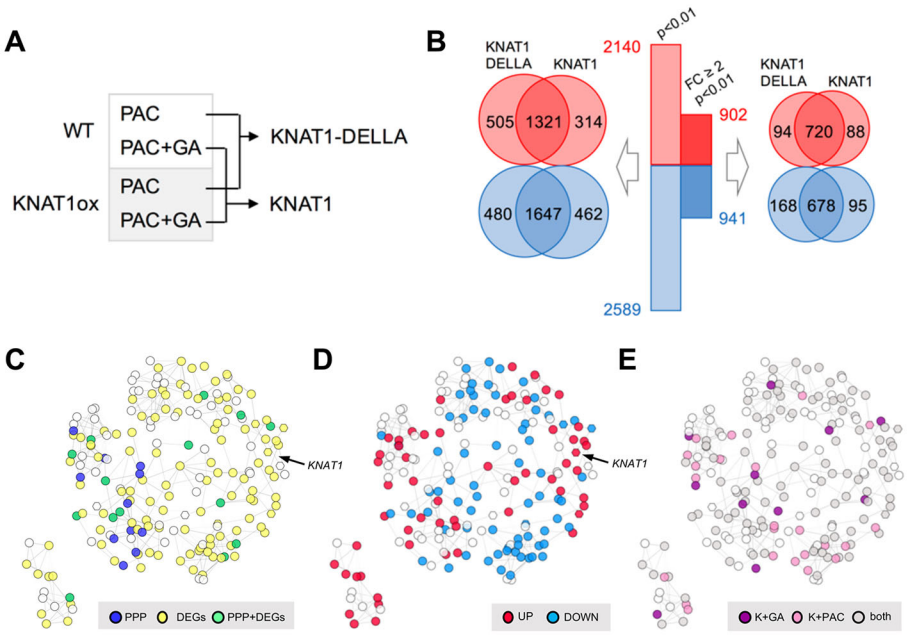

Fig. 3. Transcriptomic analysis of KNAT1 targets. (A) Experimental setup. Seven-day-old wild-type and *35S::KNAT1* seedlings incubated with 10 µM PAC for 18 h were maintained in PAC or transferred to 10 µM PAC+100 µM GA_3 for 5 h and samples were collected for RNA-seq. The comparison between PAC samples (KNAT1-DELLA) renders KNAT1 targets in the presence of DELLA proteins, whereas the comparison between PAC+GA samples (KNAT1) renders KNAT1 targets in the absence of DELLAs. (B) Diagrams showing the number of differentially expressed genes (DEGs) in *35S::KNAT1* versus wild type with statistical support (P<0.01). On the right, only DEGs with a fold change (FC) ≥2 are shown. Red and blue indicate up- and downregulation, respectively. (C-E) Co-expression network of vascular-related genes (Wang et al., 2012) misregulated in *35S::KNAT1*. In C, blue and green nodes represent phenylpropanoid metabolism genes, whereas green and yellow nodes are genes misregulated in *35S::KNAT1*. In D, red and blue indicate up- and downregulated genes, respectively, in *35S::KNAT1*. In E, purple and pink represent genes whose expression is regulated by KNAT1 only with or only without GA, respectively, whereas gray nodes are GA independent. PPP, phenylpropanoid pathway.

post-transcriptional modulation of KNAT1 activity through physical interaction with DELLAs.

Finally, to confirm that the observed xylem differentiation phenotype implied the alteration of fiber production, we carried out expression analyses of *NST1*, *NST3* and *SND2*, master regulators of secondary cell wall production during xylem fiber development (Mitsuda et al., 2007, 2005; Zhong et al., 2006). As expected, the expression of the three genes was reduced in *bp-11*, and relatively increased in *35S::KNAT1* (Fig. 5), in agreement with the observed effects on actual fiber production (Fig. 4). Similarly, PAC-dependent DELLA accumulation prevented the induction of *NST1* by KNAT1, and even caused an 85% decrease in *NST3* expression both in wild-type and *35S::KNAT1* plants (Fig. 5). Consistent with KNAT1 acting downstream of DELLAs, altering GA levels did not significantly alter the expression of these genes in the *bp-11* mutant. As NST1 and NST3 have been shown to upregulate a number of MYB transcription factors that regulate secondary cell wall developmental aspects during fiber development (including lignin biosynthesis) (Ohashi-Ito et al., 2010; Zhong et al., 2008), the effect of altering DELLA levels, i.e. by PAC or GA treatments, on *NST1* and *NST3* expression is in agreement with the role of KNAT1 in lignin biosynthesis and the enrichment of these genes among the DELLA-dependent KNAT1 targets set (Fig. 3; Fig. S5).

In conclusion, we propose that KNAT1-mediated xylem fiber development is negatively regulated by physical interaction with DELLA proteins. Given that DELLA protein levels have been shown to vary under different environmental conditions (Achard et al., 2006, 2007, 2008; Arana et al., 2011; Djakovic-Petrovic et al., 2007), it will be interesting to ascertain whether the mechanism proposed here mediates the regulation of specific aspects of cambial activity by the environment, and also whether this module regulates the development of other organs where KNAT1 and DELLAs are co-expressed, e.g. the shoot apical meristem (Hay and Tsiantis, 2010).

MATERIALS AND METHODS

Plant material and growth conditions

Arabidopsis thaliana accessions Col-0 and No-0 were used as wild type. The *bp-11* mutant and the *KNAT1ox* (*35S::KNAT1*) line have been previously described (Lincoln et al., 1994; Venglat et al., 2002). The reporter lines *RGA::GFP-RGA* and *KNAT1::KNAT1-2xeCFP* in the Col-0 background have also been generated elsewhere (Silverstone et al., 2001; Rast-Somssich et al., 2015). Seeds were stratified in water for 3 days at 4°C, sown on pots containing soil mix (1:1:1 perlite, vermiculite and peat) and grown in growth chambers under long-day conditions (16 h of light and 8 h of darkness). For vascular phenotype analysis and RT-qPCR experiments, plants were watered with 50 µM GA_3 (Sigma), 10 µM PAC (Duchefa) or mock solution once a week.

For *in vitro* growth, seeds were surface sterilized and sown on half-strength MS (Duchefa) plates with 1% (w/v) sucrose, 8 g/l agar (pH 5.7). Seeds were stratified for 3-5 days at 4°C, and grown in growth chambers under continuous light (50-60 µmol m^{-2} s^{-1}) at 22°C.

Yeast two-hybrid assays

A pENTR vector carrying the coding sequence (CDS) of *KNAT1* was obtained from SALK Institute, and transferred via LR clonase II (Invitrogen) into the pGADT7 (Clontech) yeast two-hybrid vector to create a *GAL4*-activation domain fusion. GAI deletions and the truncated version of RGA without the DELLA domain (RG52) (Gallego-Bartolomé et al., 2012) were fused to the *GAL4*-binding domain of pGBKT7 (Clontech) yeast two-hybrid vector. Direct interaction assays in yeast were carried out following

Development (2018) 145, dev164962. doi:10.1242/dev.164962

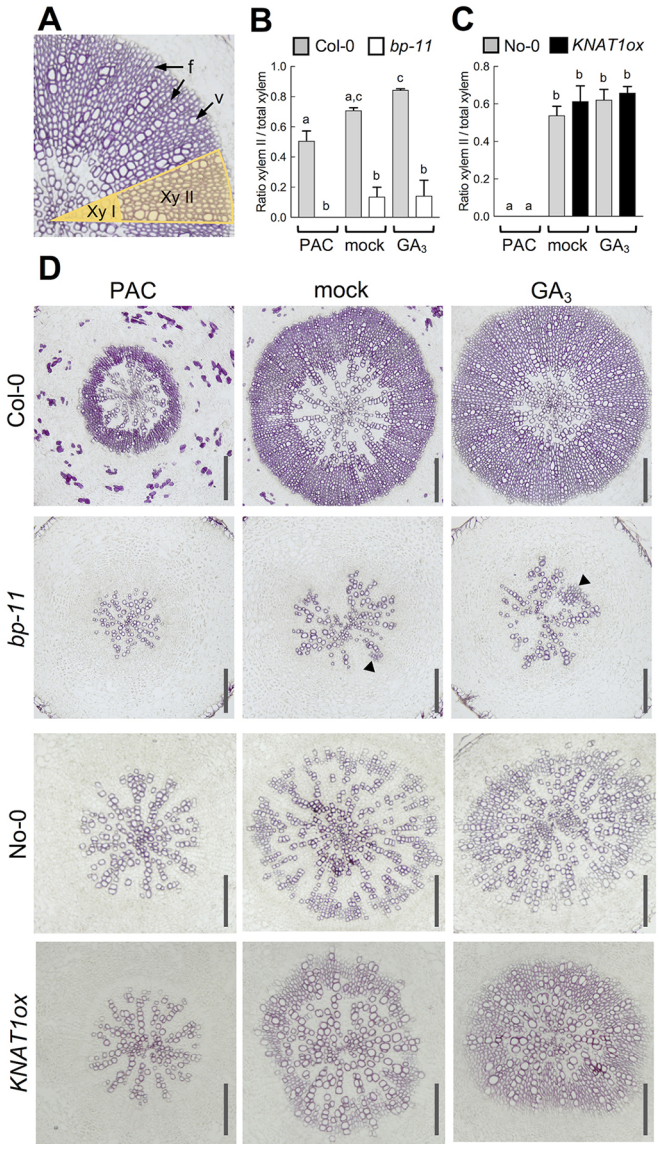

Fig. 4. Vascular phenotype of *KNAT1* loss- and gain-of-function mutants. (A) Estimation of secondary growth as the ratio between Xylem II (Xy II) and total xylem area. Although vessel elements (v) are produced during secondary growth, most of the cells produced in this phase are fibers (f). (B,C) Quantification of the ratio between Xylem II and total xylem area in 35-day-old (Col-0 and *bp-11*) (B) and 28-day-old [No-0 and *35S::KNAT1* (*KNAT1ox*)] (C) plants grown in long days in the presence of 10 µM PAC, 50 µM GA_3 or mock solution. Error bars are the s.d. of six biological replicates. Values with different letters show significant differences at $P<0.05$ according to ANOVA with Tukey's HSD test. (D) Representative sections of hypocotyls of the analyzed genotypes and conditions, stained with phloroglucinol. Arrowheads mark fiber cells in *bp-11*. Scale bars: 200 µm.

the Clontech small-scale yeast transformation procedure. Yeast strain Y187 was transformed with *GAL4*-activation domain constructs, whereas yeast strain Y2HGold was transformed with GAL4-binding domain constructs. Diploid cells with both plasmids were obtained by mating and selected in SD/-Leu/-Trp/-His and with 3-aminotriazol (3-AT) (Sigma) to test interactions.

Co-immunoprecipitation assays and western blot analysis

A pENTR vector carrying *M5GAI* has been previously described (Gallego-Bartolomé et al., 2012). For the co-immunoprecipitation assay in *Nicotiana benthamiana*, *M5GAI* and *KNAT1* CDS were transferred via LR clonase II (Invitrogen) into *pEarleyGate-203* and *-201* to create the *myc*-M5GAI and HA-KNAT1 fusions, respectively. Each construct was introduced into *Agrobacterium tumefaciens* C58 cells that were used to infiltrate *N. benthamiana* leaves. Discs from infiltrated leaves were collected after 3 days, and proteins were extracted in a buffer containing 50 mM Tris-HCl (pH 7.5), 1× protease inhibitor cocktail (Roche), 0.1% Nonidet P-40 and 10% (v/v) glycerol. Total proteins were then incubated with anti-myc paramagnetic beads (Miltenyi) for 2 h at 4°C under slight rotation. The remaining steps were conducted following manufacturer's instructions. *myc*-GAI detection was performed by using a 1:1000 dilution of anti-*myc* antibody (clone 9E10; Roche); *HA*-KNAT1 was detected by using a 1:5000 dilution of anti-HA antibody (clone 3F10; Roche). RGA immunodetection was performed using a 1:1000 dilution of polyclonal anti-RGA antibodies (Agrisera) that specifically recognize this *Arabidopsis* DELLA protein (Crocco et al., 2015).

Gene expression analysis

For RNA-sequencing (RNA-seq) analysis, 7-day-old wild-type (No-0) and *35S::KNAT1* seedlings growing in ½ MS plates under continuous light as described above were transferred to a liquid growing medium supplemented with 10 µM PAC for 18 h. Seedlings were then incubated with 10 µM PAC+ 100 µM GA_3 or maintained in 10 µM PAC for 5 h. Three biological replicates were collected for RNA-seq.

Total RNA was extracted with RNeasy Plant Mini Kit (Qiagen) according to manufacturer's instructions, treated with the DNase Kit (Ambion), and then frozen at −80°C until analyzed. The RNA concentration and integrity (RIN) were measured in a RNA nanochip (Bioanalyzer, Agilent Technologies 2100). The preparation of the libraries and the sequencing were carried out by the Genomic Service of the University of Valencia (Spain). RNA-seq libraries were generated using the TruSeq Stranded mRNA Sample Preparation Low Sample (LS) Protocol (Illumina) and sequenced on a NextSeq 500 sequencer (Illumina) with a depth of 10 M. To estimate expression levels, the RNA-seq reads were pre-processed to eliminate adapters by using the package Trim.fastaq and then mapped to the *Arabidopsis* reference genome using TopHat (Trapnell et al., 2012). Transcript counts were calculated with HTSeq-count software (Anders et al., 2015). Differentially expressed genes were determined with DESeq2 (Love et al., 2014) and edgeR packages (Robinson et al., 2010) using as criteria fold change ≥2 and $P<0.01$.

For RT-qPCR, RNA from 28- or 35-day-old plants grown under long-day conditions as described above was extracted and treated with a DNase Kit (Ambion) to eliminate genomic DNA. Poly(dT) cDNA was prepared from 1.5 µg of total RNA with PrimeScript 1st strand cDNA Synthesis Kit (Takara Bio) and analyzed on 7500 Fast Real-Time PCR System (Applied Biosystems) with SYBR Premix Ex Taq II (Tli RNaseH Plus) ROX plus (Takara Bio) according to the manufacturer's instructions. All individual reactions were carried out in triplicate. Expression levels were normalized to those of *ACT8*. Primer sequences are shown in Table S3.

Electrophoretic mobility shift assays (EMSAs)

The 6xHis-KNAT1 recombinant protein in the *pHGWA* vector was expressed in the BL21 Rosetta 2 (DE3) pLysS (Novagen) *E. coli* strain with auto-inducible medium (ZYM5052) for 24 h at 25°C. It was then purified by binding onto a HisTrap HP column (GE Healthcare Life Sciences) and eluted with imidazole. The 6xHis-MBP-RGA recombinant protein was co-expressed with the chaperone Tig in BL21 cells carrying the pTf16 plasmid (Takara) and induced with 0.1 mM IPTG for 16 h at 12°C, purified by binding onto a MBP-Trap HP column (GE Healthcare Life Sciences) and eluted with maltose. The elution buffer was replaced by EMSA buffer [15 mM HEPES-KOH (pH 7.5); 40 mM KCl; 0.1 mM dithiothreitol; 10% glycerol] by filtration through a Sephadex-G25 HiTrap column (GE Healthcare Life Sciences). Oligonucleotide probes were labeled by filling the ends with the Klenow enzyme (Fermentas) in the presence of ^{32}P-dCTP. The EMSA reaction was performed with 1 ng of ^{32}P-labeled probe, 2 µg of poly(dI-dC) and 100 ng of KNAT1 alone or combined with RGA or MBP (1:5 to 1:20 ratio as indicated), and incubated at room temperature for 20 min. The binding reactions were analyzed by

Development (2018) 145, dev164962. doi:10.1242/dev.164962

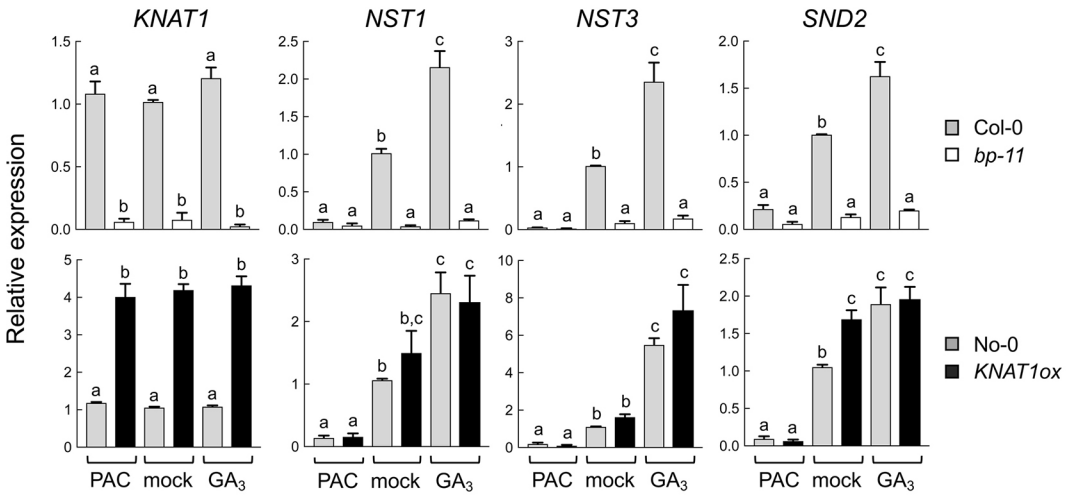

Fig. 5. Expression of fiber-differentiation master genes in *KNAT1* loss- and gain-of-function mutants. Hypocotyls of 35-day-old (Col-0 and *bp-11*) and 28-day-old [No-0 and *35S::KNAT1* (*KNAT1ox*)] plants grown in long days in the presence of 10 µM PAC, 50 µM GA_3 or mock solution were collected, and the expression of *KNAT1*, *NST1*, *NST3* and *SND2* was measured by RT-qPCR. Error bars are the s.d. of three biological replicates with three technical replicates each. Values with different letters show significant differences at $P<0.05$ according to an ANOVA with Tukey's HSD test.

electrophoresis on 6% native acrylamide gel in 0.5×TBE buffer. The gels were then dried and autoradiographed at −80°C overnight.

Microscopy analysis

Vascular phenotype of hypocotyls was analyzed with phloroglucinol staining. Briefly, hypocotyls were fixed in FAE solution (5% formaldehyde, 10% acetic acid, 50% ethanol) by vacuum infiltration for 5 min. Samples were then dehydrated through ethanol solutions up to 70% ethanol, embedded in paraffin wax using a Leica TP1020 tissue processor, sectioned using a Microm microtome and mounted on slides. Slides were placed in histoclear for 10 min for paraffin removal and then incubated 2×5 min in absolute ethanol. Samples were stained with a saturated 150 mM solution of phloroglucinol (Sigma-Aldrich) for 2 min and then soaked in 50% (v/v) HCl. Photographs were taken immediately with a Leica DM5000B microscope and a Leica DFC550 digital camera. Quantification of secondary growth was carried out as previously described (Liebsch et al., 2014) through the xylem II/total xylem ratio using ImageJ software.

Confocal microscopy

Arabidopsis lines expressing *GFP-RGA* and *KNAT1-CFP* were crossed and plants homozygous for both reporters were used for analysis. Plants were grown for 4 weeks. In order to promote DELLA accumulation, watering was supplied with 10 µM paclobutrazol (Duchefa) once the plants had developed the first pair of true leaves. Hypocotyls were hand cut with a razor blade and fixed with 4% paraformaldehyde, cleared with ClearSee solution (Kurihara et al., 2015) and stained with Direct Red 23 (Pontamine Fast Scarlet 4B, Sigma) as described by Ursache et al. (2018) with minor modifications. Cleared and stained hypocotyl sections were then placed into a drop of ClearSee on 0.3 mm cavity slides for imaging with a Zeiss LSM 780 confocal microscope. eCFP and GFP/Direct Red 23 were sequentially visualized after excitation with 405 and 488 nm laser lines, respectively. Emission filters were set to 466-481 nm for eCFP, 503-517 nm for GFP and 594-613 nm for Direct Red 23. Emission spectra for eCFP and GFP were verified within individual nuclei with the 'lambda scan' mode of the microscope.

Acknowledgements

We are grateful to Javier Forment (IBMCP, Valencia, Spain) for his help with the RNA-seq analysis, and to David Esteve-Bruna (IBMCP, Valencia, Spain) for insightful comments on the manuscript and technical help. We also thank Miltos Tsiantis (MPZI, Cologne, Germany) for seeds of the *Arabidopsis* line expressing a CFP-tagged version of KNAT1.

Competing interests

The authors declare no competing or financial interests.

Author contributions

Conceptualization: M.A.B., D.A.; Methodology: N.B.; Validation: C.Ú.; Formal analysis: A.F.-B., C.Ú., N.B.-T., J.A.; Investigation: A.F.-B., C.Ú., N.B.-T., A.S.-M., N.B., P.A., J.A.; Writing - original draft: J.A., M.A.B.; Writing - review & editing: A.F.-B., C.Ú., N.B.-T., M.A.B., D.A.; Visualization: C.Ú.; Supervision: M.A.B., D.A.; Project administration: M.A.B.; Funding acquisition: M.A.B., D.A.

Funding

This work was funded by the Ministerio de Ciencia y Tecnología (BFU2016-80621-P, BIO2016-71933-P and BIO2016-79147-R to M.A.B., D.A. and J.A., respectively). A.F-B. and N.B-T. were recipients of a Ministerio de Economía y Competitividad FPI Fellowships (BES-2011-045689 and BES-2014-068868, respectively), and A.S.-M. and M.A.B. acknowledge funding from the European Union (H2020-MSCA-IF-2016-746396). J.A. is supported by a Ramon y Cajal contract from the Ministerio de Economía y Competitividad (RYC-2014-15752).

Data availability

RNAseq data have been deposited in GEO under accession number GSE122617.

Supplementary information

Supplementary information available online at
http://dev.biologists.org/lookup/doi/10.1242/dev.164962.supplemental

References

Achard, P., Cheng, H., De Grauwe, L., Decat, J., Schoutteten, H., Moritz, T., Van Der Straeten, D., Peng, J. and Harberd, N. P. (2006). Integration of plant responses to environmentally activated phytohormonal signals. *Science* **311**, 91-94.

Achard, P., Liao, L., Jiang, C., Desnos, T., Bartlett, J., Fu, X. and Harberd, N. P. (2007). DELLAs contribute to plant photomorphogenesis. *Plant Physiol.* **143**, 1163-1172.

Achard, P., Gong, F., Cheminant, S., Alioua, M., Hedden, P. and Genschik, P. (2008). The cold-inducible CBF1 factor-dependent signaling pathway modulates the accumulation of the growth-repressing DELLA proteins via its effect on gibberellin metabolism. *Plant Cell* **20**, 2117-2129.

Aloni, R. (2013). Role of hormones in controlling vascular differentiation and the mechanism of lateral root initiation. *Planta* **238**, 819-830.

Anders, S., Pyl, P. T. and Huber, W. (2015). HTSeq–a Python framework to work with high-throughput sequencing data. *Bioinformatics* **31**, 166-169.

Arana, M. V., Marin-de la Rosa, N., Maloof, J. N., Blazquez, M. A. and Alabadi, D. (2011). Circadian oscillation of gibberellin signaling in Arabidopsis. *Proc. Natl. Acad. Sci. US A* **108**, 9292-9297.

Byrne, M. E., Simorowski, J. and Martienssen, R. A. (2002). ASYMMETRIC LEAVES1 reveals knox gene redundancy in Arabidopsis. *Development* **129**, 1957-1965.

Crocco, C. D., Locascio, A., Escudero, C. M., Alabadí, D., Blázquez, M. A. and Botto, J. F. (2015). The transcriptional regulator BBX24 impairs DELLA activity to promote shade avoidance in Arabidopsis thaliana. *Nat. Commun.* **6**, 6202.

Daviere, J.-M. and Achard, P. (2013). Gibberellin signaling in plants. *Development* **140**, 1147-1151.
de Lucas, M., Davière, J.-M., Rodríguez-Falcón, M., Pontin, M., Iglesias-Pedraz, J. M., Lorrain, S., Fankhauser, C., Blazquez, M. A., Titarenko, E. and Prat, S. (2008). A molecular framework for light and gibberellin control of cell elongation. *Nature* **451**, 480-484.
Djakovic-Petrovic, T., de Wit, M., Voesenek, L. A. C. J. and Pierik, R. (2007). DELLA protein function in growth responses to canopy signals. *Plant J.* **51**, 117-126.
Eriksson, M. E., Israelsson, M., Olsson, O. and Moritz, T. (2000). Increased gibberellin biosynthesis in transgenic trees promotes growth, biomass production and xylem fiber length. *Nat. Biotechnol.* **18**, 784-788.
Fukazawa, J., Teramura, H., Murakoshi, S., Nasuno, K., Nishida, N., Ito, T., Yoshida, M., Kamiya, Y., Yamaguchi, S. and Takahashi, Y. (2014). DELLAs function as coactivators of GAI-ASSOCIATED FACTOR1 in regulation of gibberellin homeostasis and signaling in Arabidopsis. *Plant Cell* **26**, 2920-2938.
Gallego-Bartolomé, J., Minguet, E. G., Grau-Enguix, F., Abbas, M., Locascio, A., Thomas, S. G., Alabadí, D. and Blázquez, M. A. (2012). Molecular mechanism for the interaction between gibberellin and brassinosteroid signaling pathways in Arabidopsis. *Proc. Natl. Acad. Sci. USA* **109**, 13446-13451.
Hay, A. and Tsiantis, M. (2010). KNOX genes: versatile regulators of plant development and diversity. *Development* **137**, 3153-3165.
Hirano, K., Ueguchi-Tanaka, M. and Matsuoka, M. (2008). GID1-mediated gibberellin signaling in plants. *Trends Plant Sci.* **13**, 192-199.
Hou, X., Lee, L. Y. C., Xia, K., Yan, Y. and Yu, H. (2010). DELLAs modulate jasmonate signaling via competitive binding to JAZs. *Dev. Cell* **19**, 884-894.
Ikematsu, S., Tasaka, M., Torii, K. U. and Uchida, N. (2017). ERECTA-family receptor kinase genes redundantly prevent premature progression of secondary growth in the Arabidopsis hypocotyl. *New Phytol.* **213**, 1697-1709.
Kurihara, D., Mizuta, Y., Sato, Y. and Higashiyama, T. (2015). ClearSee: a rapid optical clearing reagent for whole-plant fluorescence imaging. *Development* **142**, 4168-4179.
Liebsch, D., Sunaryo, W., Holmlund, M., Norberg, M., Zhang, J., Hall, H. C., Helizon, H., Jin, X., Helariutta, Y., Nilsson, O. et al. (2014). Class I KNOX transcription factors promote differentiation of cambial derivatives into xylem fibers in the Arabidopsis hypocotyl. *Development* **141**, 4311-4319.
Lim, S., Park, J., Lee, N., Jeong, J., Toh, S., Watanabe, A., Kim, J., Kang, H., Kim, D. H., Kawakami, N. et al. (2013). ABA-INSENSITIVE3, ABA-INSENSITIVE5, and DELLAs interact to activate the expression of SOMNUS and other high-temperature-inducible genes in imbibed seeds in arabidopsis. *Plant Cell* **25**, 4863-4878.
Lincoln, C., Long, J., Yamaguchi, J., Serikawa, K. and Hake, S. (1994). A knotted1-like homeobox gene in Arabidopsis is expressed in the vegetative meristem and dramatically alters leaf morphology when overexpressed in transgenic plants. *Plant Cell* **6**, 1859-1876.
Locascio, A., Blázquez, M. A. and Alabadí, D. (2013a). Dynamic regulation of cortical microtubule organization through prefoldin-DELLA interaction. *Curr. Biol.* **23**, 804-809.
Locascio, A., Blázquez, M. A. and Alabadí, D. (2013b). Genomic analysis of della protein activity. *Plant Cell Physiol.* **54**, 1229-1237.
Love, M. I., Huber, W. and Anders, S. (2014). Moderated estimation of fold change and dispersion for RNA-seq data with DESeq2. *Genome Biol.* **15**, 550.
Marin-de la Rosa, N., Sotillo, B., Miskolczi, P., Gibbs, D. J., Vicente, J., Carbonero, P., Onate-Sanchez, L., Holdsworth, M. J., Bhalerao, R., Alabadi, D. et al. (2014). Large-scale identification of gibberellin-related transcription factors defines Group VII ETHYLENE RESPONSE FACTORS as functional DELLA partners. *Plant Physiol.* **166**, 1022-1032.
Marin-de la Rosa, N., Pfeiffer, A., Hill, K., Locascio, A., Bhalerao, R. P., Miskolczi, P., Gronlund, A. L., Wanchoo-Kohli, A., Thomas, S. G., Bennett, M. J. et al. (2015). Genome wide binding site analysis reveals transcriptional coactivation of cytokinin-responsive genes by DELLA proteins. *PLoS Genet.* **11**, e1005337.
Mauriat, M. and Moritz, T. (2009). Analyses of GA20ox- and GID1-over-expressing aspen suggest that gibberellins play two distinct roles in wood formation. *Plant J.* **58**, 989-1003.
Mele, G., Ori, N., Sato, Y. and Hake, S. (2003). The knotted1-like homeobox gene BREVIPEDICELLUS regulates cell differentiation by modulating metabolic pathways. *Genes Dev.* **17**, 2088-2093.
Mitsuda, N., Seki, M., Shinozaki, K. and Ohme-Takagi, M. (2005). The NAC transcription factors NST1 and NST2 of Arabidopsis regulate secondary wall thickening and are required for anther dehiscence. *Plant Cell* **17**, 2993-3006.
Mitsuda, N., Iwase, A., Yamamoto, H., Yoshida, M., Seki, M., Shinozaki, K. and Ohme-Takagi, M. (2007). NAC transcription factors, NST1 and NST3, are key regulators of the formation of secondary walls in woody tissues of Arabidopsis. *Plant Cell* **19**, 270-280.
Obayashi, T., Kinoshita, K., Nakai, K., Shibaoba, M., Hayashi, S., Saeki, M., Shibata, D., Saito, K. and Ohta, H. (2007). ATTED-II: a database of co-expressed genes and cis elements for identifying co-regulated gene groups in Arabidopsis. *Nucleic Acid Res.* **35**, D863-D869.
Ohashi-Ito, K., Oda, Y. and Fukuda, H. (2010). Arabidopsis VASCULAR-RELATED NAC-DOMAIN6 directly regulates the genes that govern programmed cell death and secondary wall formation during xylem differentiation. *Plant Cell* **22**, 3461-3473.
Pattanaik, S., Patra, B., Singh, S. K. and Yuan, L. (2014). An overview of the gene regulatory network controlling trichome development in the model plant, Arabidopsis. *Front. Plant Sci.* **5**, 259.
Ragni, L., Nieminen, K., Pacheco-Villalobos, D., Sibout, R., Schwechheimer, C. and Hardtke, C. S. (2011). Mobile gibberellin directly stimulates Arabidopsis hypocotyl xylem expansion. *Plant Cell* **23**, 1322-1336.
Rast-Somssich, M. I., Broholm, S., Jenkins, H., Canales, C., Vlad, D., Kwantes, M., Bilsborough, G., Dello Ioio, R., Ewing, R. M., Laufs, P. et al. (2015). Alternate wiring of a KNOXI genetic network underlies differences in leaf development of A. thaliana and C. hirsuta. *Genes Dev.* **29**, 2391-2404.
Resentini, F., Felipo-Benavent, A., Colombo, L., Blázquez, M. A., Alabadí, D. and Masiero, S. (2015). TCP14 and TCP15 mediate the promotion of seed germination by gibberellins in Arabidopsis thaliana. *Mol. Plant* **8**, 482-485.
Robinson, M. D., McCarthy, D. J. and Smyth, G. K. (2010). edgeR: a Bioconductor package for differential expression analysis of digital gene expression data. *Bioinformatics* **26**, 139-140.
Rombolá-Caldentey, B., Rueda-Romero, P., Iglesias-Fernández, R., Carbonero, P. and Oñate-Sánchez, L. (2014). Arabidopsis DELLA and two HD-ZIP transcription factors regulate GA signaling in the epidermis through the L1 box cis-element. *Plant Cell* **26**, 2905-2919.
Schwechheimer, C. (2011). Gibberellin signaling in plants-the extended version. *Front. Plant Sci.* **2**, 107.
Shu, K., Liu, X.-D., Xie, Q. and He, Z.-H. (2016). Two faces of one seed: hormonal regulation of dormancy and germination. *Mol. Plant* **9**, 34-45.
Silverstone, A. L., Ciampaglio, C. N. and Sun, T. (1998). The Arabidopsis RGA gene encodes a transcriptional regulator repressing the gibberellin signal transduction pathway. *Plant Cell* **10**, 155-169.
Silverstone, A. L., Jung, H. S., Dill, A., Kawaide, H., Kamiya, Y. and Sun, T. P. (2001). Repressing a repressor: gibberellin induced rapid reduction of the RGA protein in Arabidopsis. *Plant Cell* **13**, 1555-1566.
Trapnell, C., Roberts, A., Goff, L., Pertea, G., Kim, D., Kelley, D. R., Pimentel, H., Salzberg, S. L., Rinn, J. L. and Pachter, L. (2012). Differential gene and transcript expression analysis of RNA-seq experiments with TopHat and Cufflinks. *Nat. Protoc.* **7**, 562-578.
Ursache, R., Andersen, T. G., Marhavý, P. and Geldner, N. (2018). A protocol for combining fluorescent proteins with histological stains for diverse cell wall components. *Plant J.* **93**, 399-412.
Venglat, S. P., Dumonceaux, T., Rozwadowski, K., Parnell, L., Babic, V., Keller, W., Martienssen, R., Selvaraj, G. and Datla, R. (2002). The homeobox gene BREVIPEDICELLUS is a key regulator of inflorescence architecture in Arabidopsis. *Proc. Natl. Acad. Sci. USA* **99**, 4730-4735.
Wang, S., Yin, Y., Ma, Q., Tang, X., Hao, D. and Xu, Y. (2012). Genome-scale identification of cell-wall related genes in Arabidopsis based on co-expression network analysis. *BMC Plant Biol.* **12**, 138.
Yu, S., Galvao, V. C., Zhang, Y.-C., Horrer, D., Zhang, T.-Q., Hao, Y.-H., Feng, Y.-Q., Wang, S., Schmid, M. and Wang, J.-W. (2012). Gibberellin regulates the Arabidopsis floral transition through miR156-targeted SQUAMOSA promoter binding-like transcription factors. *Plant Cell* **24**, 3320-3332.
Zhong, R., Demura, T. and Ye, Z.-H. (2006). SND1, a NAC domain transcription factor, is a key regulator of secondary wall synthesis in fibers of Arabidopsis. *Plant Cell* **18**, 3158-3170.
Zhong, R., Lee, C., Zhou, J., McCarthy, R. L. and Ye, Z.-H. (2008). A battery of transcription factors involved in the regulation of secondary cell wall biosynthesis in Arabidopsis. *Plant Cell* **20**, 2763-2782.

Table S1. Transcriptomic analysis of KNAT1 targets in the presence and absence of DELLAs.

Click here to download Table S1

Table S2. Network of Secondary Cell Wall genes controlled by KNAT1.

shared name	network_symbol	symbol	Type	BP-DELLA	Expression
At3g46660	UGT76E12	UGT76E12	BP	both	UP
At4g26320	AGP13	AGP13	BP	both	D
At4g23496	SP1L5	SP1L5	BP	both	D
At1g72260	thionin 2...	THI2.1.1	BP	both	UP
At1g52000	Mannose-bi..		BP	both	UP
At1g23760	PG3	PG3	BP	both	D
At1g60090	BGLU4	BGLU4	BP	both	UP
At5g44310	LEA		BP	both	D
At4g37990	ELI3-2	ELI3-2	BP-PHENYL	both	UP
At1g17180	GSTU25	GSTU25	BP	both	UP
At3g21370	BGLU19	BGLU19	BP-PHENYL	both	D
At3g28220	TRAF-like		BP	both	UP
At1g18710	MYB47	MYB47	BP	both	UP
At1g66860	transferas..		BP	both	D
At1g10585	DNA-bindin..		BP	both	UP
At1g52410	TSA1	TSA1	BP	both	UP
At4g24780	Pectin lya..		BP	both	D
At2g29490	GSTU1	GSTU1	BP	both	UP
At5g01840	OFP1	OFP1	BP	both	D
At3g15670	LEA		BP	both	D
At4g02270	RHS13	RHS13	BP	both	UP
At2g01610	inhibitor		BP	both	D
At4g08150	KNAT1	KNAT1	BP	both	UP
At5g10120	Ethylene i..		BP	both	D
At4g16770	2OG		BP	both	D
At3g59680			BP	both	D
At1g78970	LUP1	LUP1	BP	both	D
At4g15100	scpl30	scpl30	BP	both	D
At3g02500			BP	both	UP
At3g02885	GASA5	GASA5	BP	both	D
At3g10710	RHS12	RHS12	BP	both	UP
At3g09960	phosphoest..		BP	both	UP
At4g21650	Subtilase		BP	both	UP
At3g09220	LAC7	LAC7	BP	both	D
At4g39320	microtubul..		BP	both	D
At5g05290	EXPA2	EXPA2	BP	both	D
At5g28510	BGLU24	BGLU24	BP-PHENYL	both	D
At1g64160	DIR5		BP	both	UP
At2g20520	FLA6	FLA6	BP	both	UP
At4g14630	GLP9	GLP9	BP	both	D
At4g15093	LigB		BP	both	UP
At5g57770	DUF828		BP	both	D
At5g14090			BP	both	D
At2g41260	M17	M17	BP	both	D
At4g18510	CLE2	CLE2	BP	both	UP
At3g46490	2OG		BP	both	UP
At1g60470	GolS4	GolS4	BP	both	D
At1g48130	PER1	PER1	BP-PHENYL	both	D
At3g27400	Pectin lya..		BP	both	D
At3g29780	RALFL27	RALFL27	BP	both	D
At2g34910			BP	both	UP
At4g28250	EXPB3	EXPB3	BP	both	D
At5g39580	Peroxidase		BP-PHENYL	both	UP
At1g78490	CYP708A3	CYP708A3	BP	both	UP
At5g64100	Peroxidase		BP-PHENYL	both	UP
At3g09520	EXO70H4	EXO70H4	BP	both	D
At5g58390	Peroxidase		BP-PHENYL	both	UP
At4g08780	Peroxidase		BP-PHENYL	both	D
At2g36570	kinase		BP	both	D
At4g20210	transferas..		BP	both	D
At1g75830	LCR67	PDF1.1	BP	both	UP
At3g62740	BGLU7	BGLU7	BP	both	D
At1g03820			BP	both	D
At4g02850	PhzC/PhzF		BP	both	D

At2g39330	JAL23	JAL23	BP	both	UP
At1g62770	inhibitor		BP	both	UP
At3g50350	DUF1685		BP	both	D
At2g46750	GulLO2		BP	both	UP
At2g18800	XTH21	XTH21	BP	both	UP
At5g17820	Peroxidase		BP-PHENYL	both	UP
At5g04230	PAL3	PAL3	BP-PHENYL	both	UP
At5g62490	HVA22B	HVA22B	BP	both	D
At5g44120	CRU1	CRU1	BP	both	D
At2g34060	Peroxidase		BP-PHENYL	both	D
At5g04330	CYP84A4		BP-PHENYL	both	D
At5g22410	RHS18	RHS18	BP-PHENYL	both	UP
At1g17170	GSTU24	GSTU24	BP	both	UP
At3g18870	transcript..		BP	both	UP
At5g47810	PFK2	PFK2	BP	both	D
At4g22460	inhibitor		BP	both	UP
At3g56300	tRNA syn		BP	both	UP
At3g13784	CWINV5	CWINV5	BP	both	D
At1g70510	KNAT2	KNAT2	BP	both	D
At3g02240	RGF7	RGF7	BP	both	D
At3g59370	Vacuolar c..		BP	both	UP
At1g64690	BLT	BLT	BP	both	D
At3g54040	PAR1		BP	both	UP
At5g48070	XTH20	XTH20	BP	both	D
At5g03120			BP	both	UP
At5g27360	SFP2	SFP2	BP	both	UP
At1g18970	GLP4	GLP4	BP	both	D
At5g28080	WNK9	WNK9	BP	both	UP
At2g29480	GSTU2	GSTU2	BP	both	UP
At3g47040	hydrolase		BP	both	UP
At2g28490	RmlC-like ..		BP	both	D
At1g73190	TIP3;1	TIP3;1	BP	both	D
At4g22212	Arabidopsi..		BP	both	UP
At3g23290	LSH4	LSH4	BP	both	UP
At4g19530	TIR-NBS-LR..		BP	both	UP
At1g12560	EXPA7	EXPA7	BP	both	D
At2g21045	phosphatas..		BP	both	UP
At4g10020	HSD5	HSD5	BP	both	D
At2g03090	EXPA15	EXPA15	BP	both	D
At4g04990	DUF761		BP	GA	D
At3g01190	Peroxidase		PHENYL	GA	
At4g19680	IRT2	IRT2	BP	GA	D
At5g04180	ACA3	ATACA3	BP	GA	D
At5g28520	Mannose-bi..		BP	GA	D
At3g25130			C	GA	
At5g06790			BP	GA	D
At3g50560	Rossmann-f..		BP	GA	D
At5g05840	DUF620		BP	GA	UP
At2g45570	CYP76C2	CYP76C2	BP	GA	UP
At5g47000	Peroxidase		PHENYL	GA	
At1g05680	UGT74E2	UGT74E2	BP	PAC	UP
At5g35190	EXT13	EXT13	BP	PAC	UP
At1g54870	Rossmann-f..		BP	PAC	D
At3g21770	Peroxidase		PHENYL	PAC	
At1g62360	WAM1	WAM1	BP	PAC	D
At1g30870	Peroxidase		PHENYL	PAC	
At2g36750	UGT73C1	UGT73C1	BP	PAC	UP
At2g35150	EXL7	EXL7	BP	PAC	D
At3g62680	PRP3	PRP3	C	PAC	
At2g25890	Oleosin		BP	PAC	D
At4g26010	Peroxidase		PHENYL	PAC	
At5g22470	transferas..		BP	PAC	D
At3g05950	RmlC-like ..		BP	PAC	D
At3g60280	UCC3	UCC3	BP	PAC	UP
At1g05510	DUF1264		BP	PAC	D

At4g21020	LEA		BP	PAC	D
At5g67400	RHS19	RHS19	BP-PHENYL	PAC	UP
At4g33720	CAP		BP	PAC	D
At5g63600	FLS5	FLS5	C	PAC	
At5g66780			BP	PAC	D
At2g37770	ChlAKR	ChlAKR	C	PAC	
At1g04560	AWPM-19-li..		BP	PAC	D
At3g21380	Mannose-bi..		BP	PAC	D
At1g16530	LBD3	LBD3	C		
At3g45700	Major faci..		C		
At3g23190	HR-like le..		C		
At2g46640			C		
At2g31180	MYB14AT	MYB14AT	C		
At5g39880			C		
At4g33730	CAP		C		
At5g19890	Peroxidase		PHENYL		
At4g12980	Auxin-resp..		C		
At4g26200	ACS7	ATACS7	C		
At5g61650	CYCP4;2	CYCP4;2	C		
At3g45410	kinase		C		
At2g42610	LSH10	LSH10	C		
At5g60760	hydrolase		C		
At3g56350	mutase		C		
At3g30340	UMAMIT32		C		
At2g15490	UGT73B4	UGT73B4	C		
At5g57530	XTH12	XTH12	C		
At5g65730	XTH6	XTH6	C		
At2g33620	DNA-bindin..		C		
At1g69230	SP1L2	SP1L2	C		
At2g19970	CAP		C		
At1g01200	RABA3	RABA3	C		
At3g47050	hydrolase		PHENYL		
At5g44400	Berberine		C		
At4g25820	XTR9	XTR9	C		
At4g14380			C		
At1g49570	Peroxidase		PHENYL		
At2g39220	PLP6	PLP6	C		
At1g54970	RHS7	RHS7	C		
At4g36430	Peroxidase		PHENYL		
At5g06730	Peroxidase		PHENYL		
At1g17810	BETA-TIP	BETA-TIP	C		
At3g46670	UGT76E11	UGT76E11	C		
At1g34330			C		
At1g27990			C		
At4g17810	zinc finge..		C		
At2g18300	HBI1		C		
At5g05500	MOP10	MOP10	C		
At1g62980	EXPA18	EXPA18	C		
At5g66815			C		
At4g20320	synthase		C		
At3g44940	DUF1635		C		
At1g64390	GH9C2	GH9C2	C		
At2g34510	DUF642		C		
At1g31320	LBD4	LBD4	C		
At2g31085	CLE6	CLE6	C		
At4g23720	DUF1191		C		
At1g66570	SUC7	SUC7	C		
At3g01420	PADOX-1	PADOX-1	C		
At2g44110	MLO15	MLO15	C		
At1g27461			C		
At5g59510	RTFL5	RTFL5	C		
At3g26610	Pectin lya..		C		
At1g54020	hydrolase		C		
At2g39560	Putative m..		C		
At1g34510	Peroxidase		PHENYL		
At4g18630	DUF688		C		
At5g25810	tny	tny	C		

Table S3. Primers used in this study.

	Fwd	Rev
KNAT1	ACCATCTGAAGACATGCAGTTCA	CCGAGACGATAAGGTCCATCA
NST1	CATTCAAGAGATGTGTAAAATAGGAACAA	GCCAGTTGCTTTCCAAAATCC
NST3	GTGTCCGGAGAATTGGACTGA	TCAGCATAGCCATTAGACATTGGA
SND2	TGATGAAGTTGTGAGCACTGAA	TGACAAGAGACCGGAAGTGA
ACT8	AGTGGTCGTACAACCGGTATT	GAGGATAGCATGTGGAAGTGA
AT2G45570/CYP76C2	CACGACAAGGTTTCCGTTG	GTCGCCGACAGTTTTCTCA
AT5G05840	TCGTGGTCCTCCTAGACCAT	GCCGTTGATTTTGGATCAAG
AT4G04990	TGTTCCTGTAAAGACTTTTCCACA	TTTCGGCTTTGACTCTCTCC
AT5G28520	AGTGGGCAACCCCAAACT	TCATCCTTTTGATCAATCTCAAAC
AT3G60280/UCC3	ACTTTCAGAGTCGGTGACACTCTA	TCATCCTTTTGATCAATCTCAAAC
AT5G35190	TTCACCTAAAAAGTATTCCCCATACTA	GGGCCTTGTCTTCTATATTGTAGTG
AT1G54870	CCGTACAAACATCTTTTCTTACTTCTT	CATTCACCGAAGTGGTGTTG
AT1G05510	CCAAATCCACCAACATCTCTG	CATTCACCGAAGTGGTGTTG

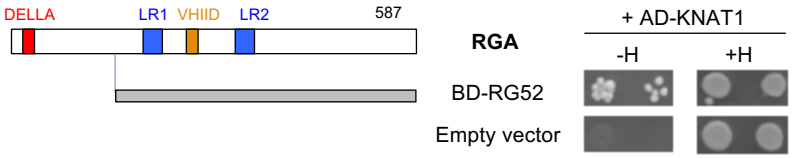

Fig S1. RGA also interacts physically with KNAT1. Y2H assay analyzing the interaction between KNAT1 and a truncated version of RGA without the DELLA domain (RG52). Two serial dilutions per yeast clone are shown. +H, control medium containing His. –H, selective medium lacking His. Pictures of the plates were taken after 5 days at 28°C.

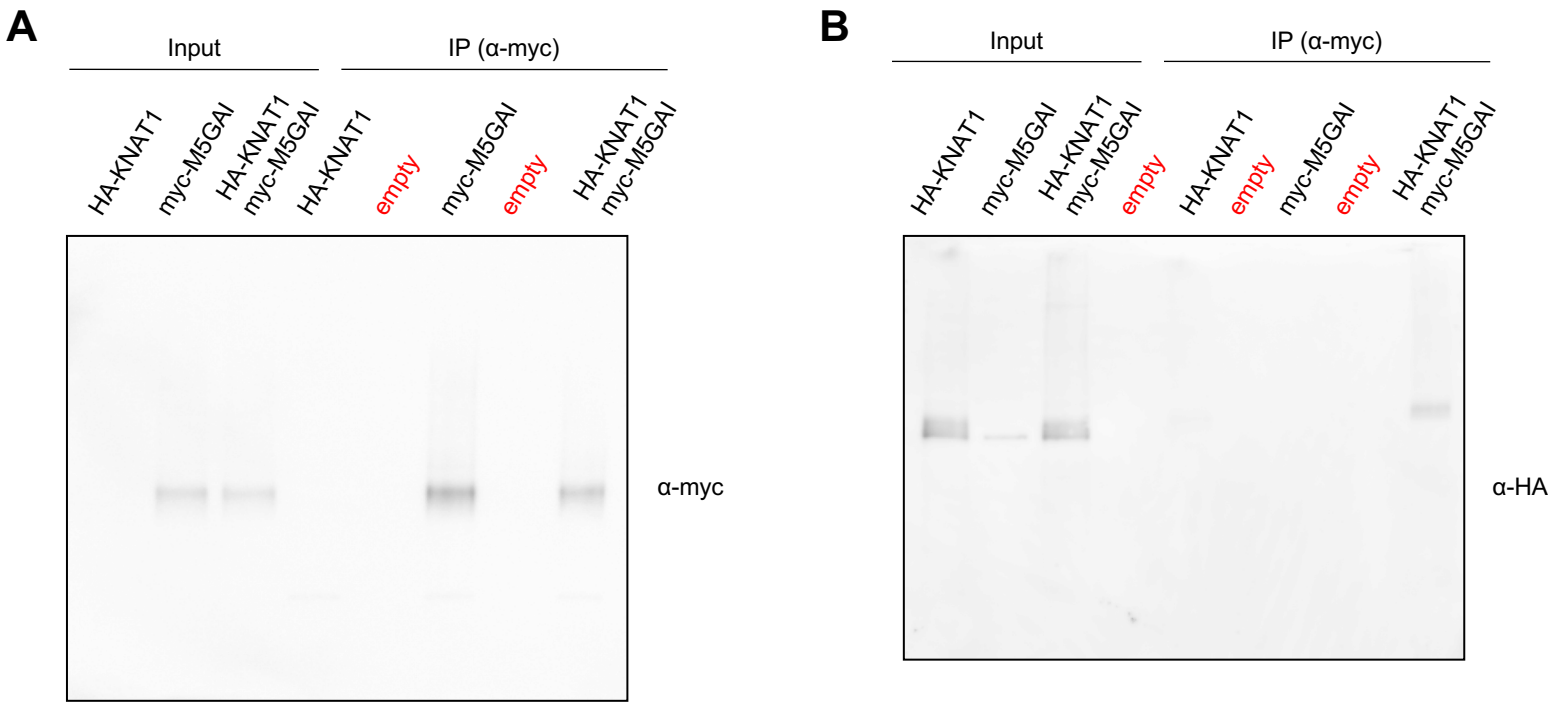

Figure S2. KNAT1 interacts physically with GAI by Co-IP. Full scanned gels for western blots with anti-myc (A) and anti-HA (B) antibodies shown in Figure 1B.

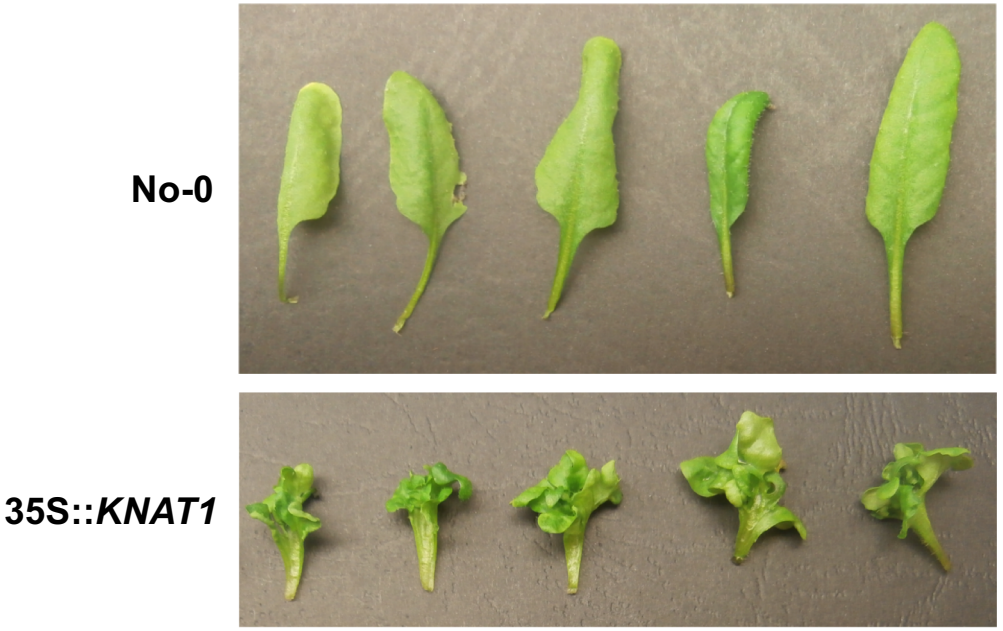

Fig S3. Leaf phenotype of *35S::KNAT1* plants. 35S::*KNAT1* plants and their parental WT (No-0) were grown in long days for 28 days and leaves 3 to 7 from one plant were dissected and photographed, as an example of the reported phenotypic alterations caused by *KNAT1* ectopic expression.

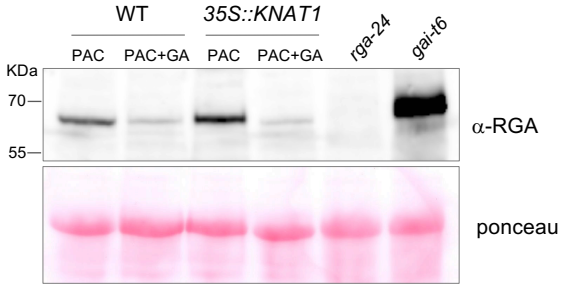

Fig S4. RGA levels after incubation of 35S::KNAT1 seedlings with paclobutrazol (PAC) and GA_3. 7-day-old wild-type and 35S::KNAT1 seedlings grown on ½ MS were treated with 10 μM PAC for 18 hours and then were maintained in PAC or transferred to 100 μM GA_3 for 5 hours. RGA protein was immunodetected using anti-RGA antibody. The specificity of the antibody against RGA was demonstrated by the lack of a 60 KDa band in the null *rga-24* mutant, while this band was clearly detected in extracts of the null *gai-t6* mutant.

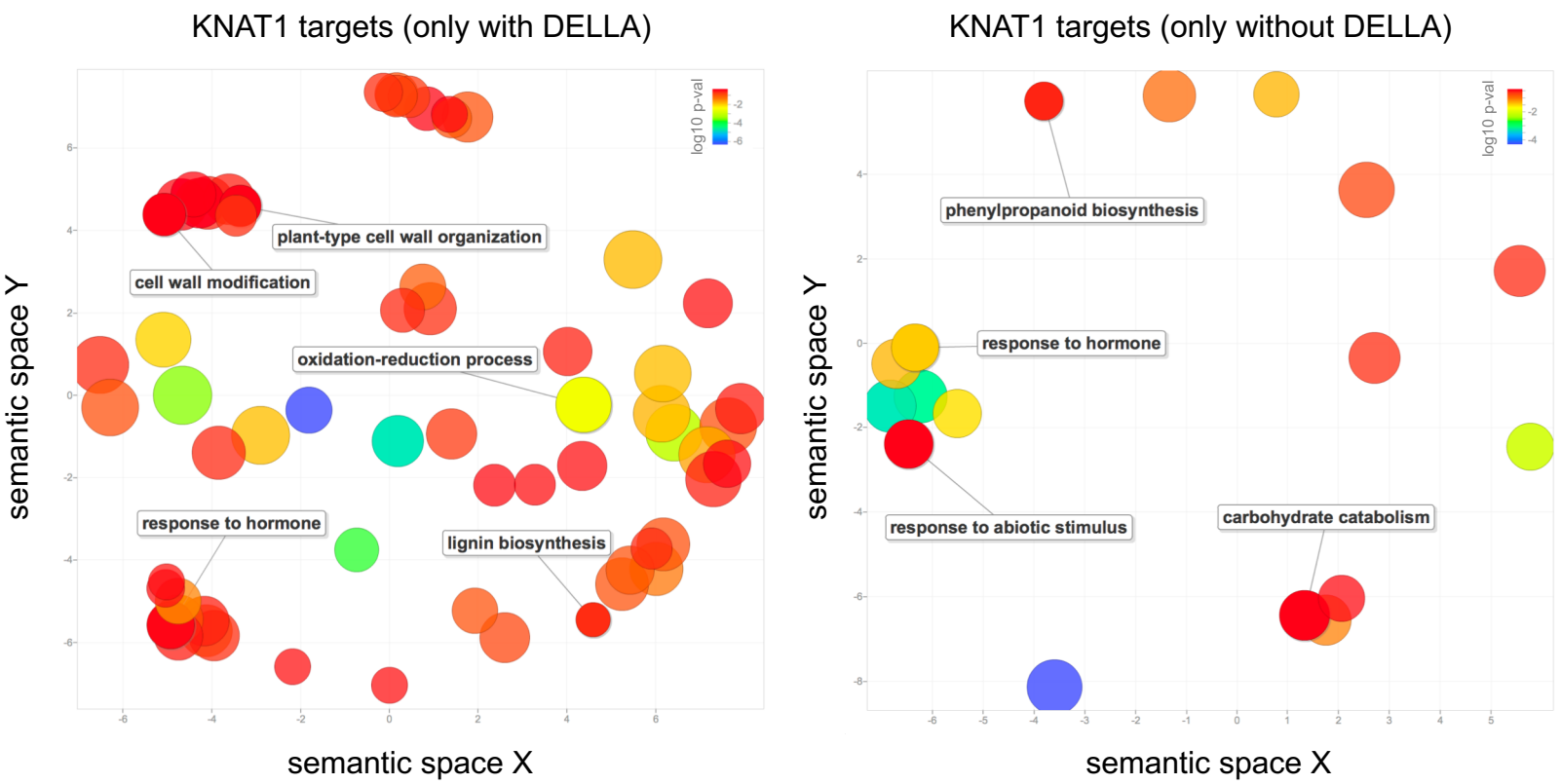

Fig S5. Gene Ontology analysis of KNAT1 targets. Statistically significant enrichment of GO categories was calculated using AgriGO (Du et al., 2010) and represented here with ReviGO (Supek et al., 2011)

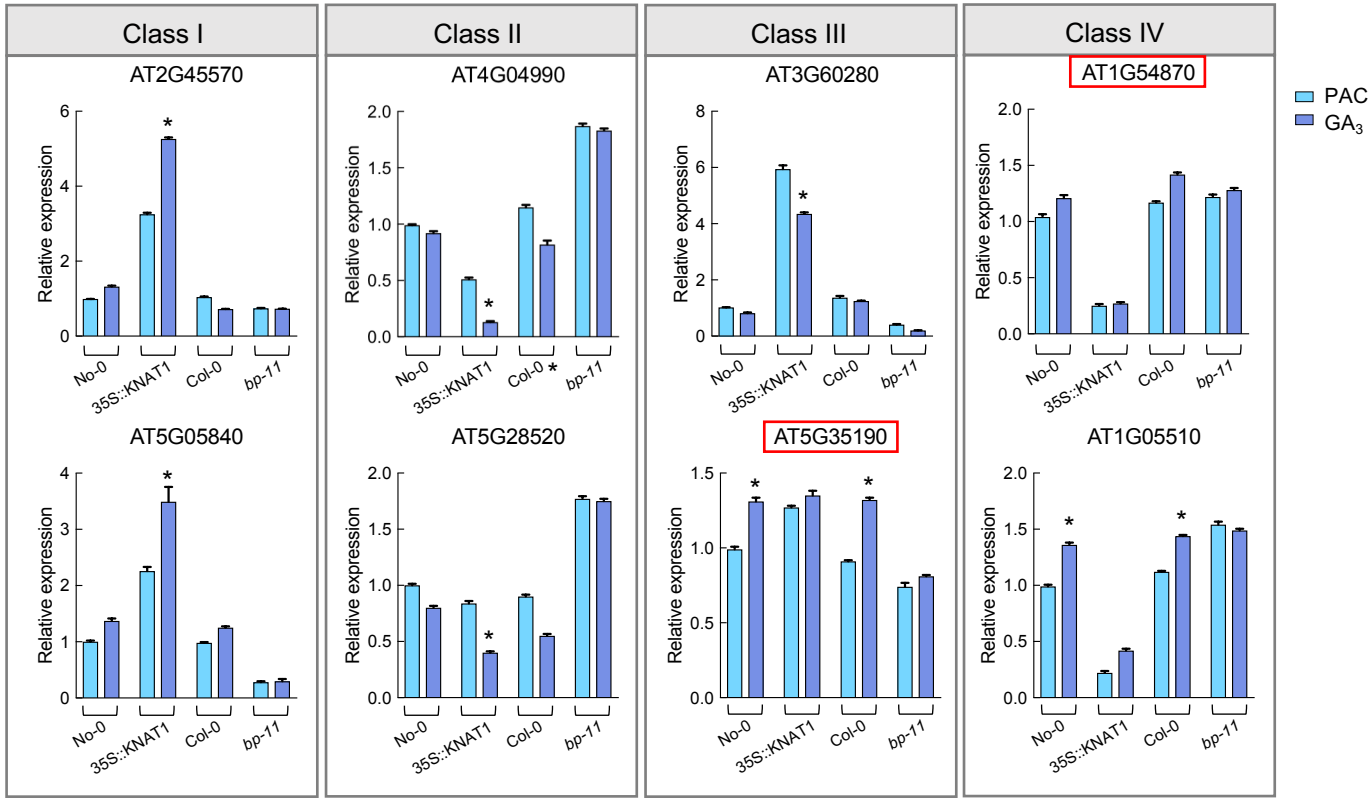

Class I: DELLAs impair induction by KNAT1
Class II: DELLAs impair repression by KNAT1
Class III: DELLAs promote induction by KNAT1
Class IV: DELLAs promote repression by KNAT1

Fig S6. Expression analysis of putative DELLA-dependent KNAT1 targets related to secondary cell walls. Hypocotyls of 28-day-old (No-0, 35S::KNAT1) and 35-day-old (Col-0, *bp-11*) plants grown in long days in the presence of 10 µM PAC or 50 µM GA_3 solution were collected and gene expression was measured by RT-qPCR. Error bars are the SD of three technical replicates. Asterisks indicate statistical significance ($p<0.05$) with respect to the PAC treatment in the same genotype. In red, genes for which the predicted joint DELLA-KNAT1 regulation does not occur.